iScience

CellPress

Article

System-Level Analysis of Lignin Valorization in Lignocellulosic Biorefineries

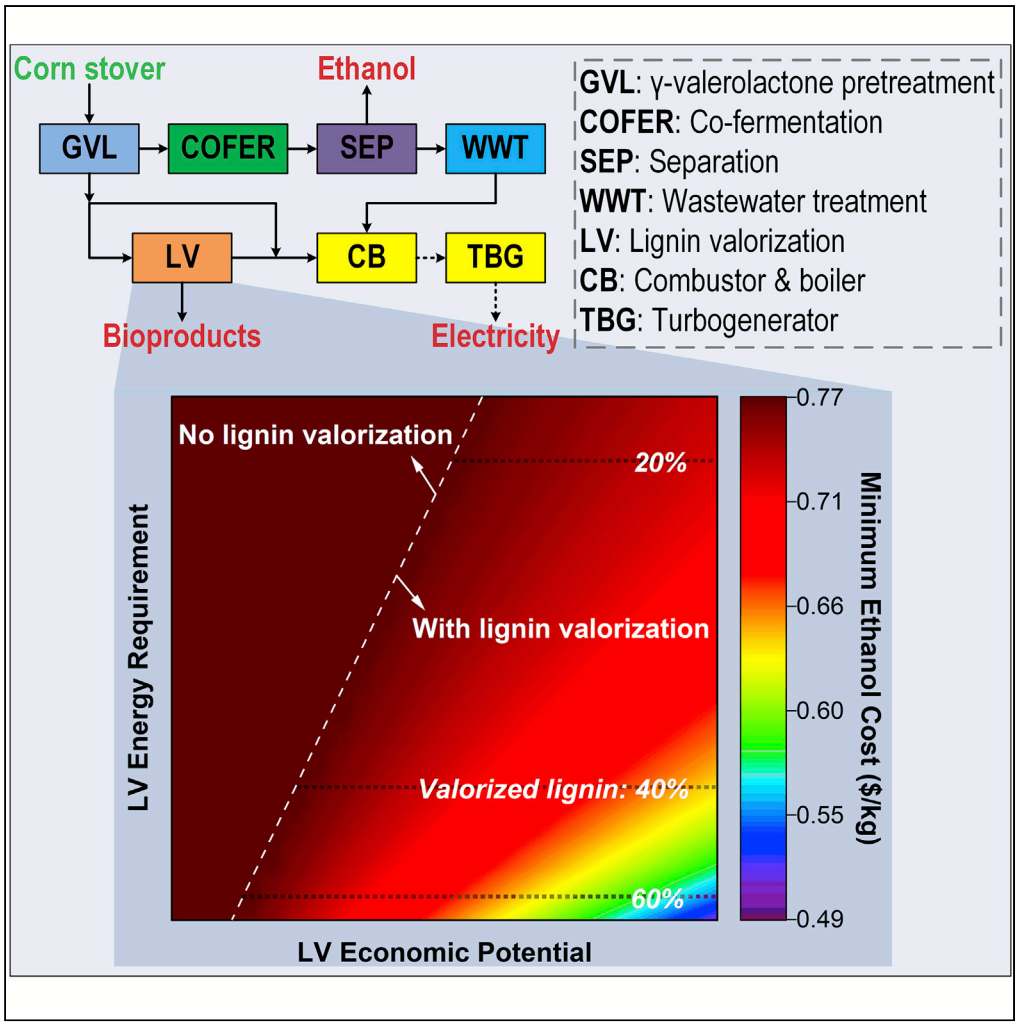

Kefeng Huang, Peyman Fasahati, Christos T. Maravelias

christos.maravelias@wisc.edu

HIGHLIGHTS

Developed optimization model to evaluate biorefinery with lignin valorization

Studied impact of technical, economic, and energy parameters on economics

Lignin utilization is optimized to achieve a thermal-neutral biorefinery

Established technology targets for economic and energetic feasibility

Huang et al., iScience 23, 100751
January 24, 2020
https://doi.org/10.1016/j.isci.2019.100751

iScience

CellPress

Article

System-Level Analysis of Lignin Valorization in Lignocellulosic Biorefineries

Kefeng Huang,[1] Peyman Fasahati,[1] and Christos T. Maravelias[1,2,*]

SUMMARY

We study the economics and energy efficiency of biorefineries employing lignin valorization. We use superstructure-based process synthesis to study different configurations under different types of constraints. Using optimization, we examine the impact of various parameters for lignin valorization such as bioproduct selling price, production cost, conversion coefficient, and energy requirement. The results show that the optimal strategy leading to a minimum ethanol selling price (MESP) of $3.44/GGE does not include lignin valorization. Results indicate that under certain scenarios, the optimal biorefinery strategies with lignin valorization tend to be energy deficient, and thus the optimal pretreatment technology may switch from γ-valerolactone-based deconstruction to ammonia fiber expansion. Further analysis is performed to study how improvements in combinations of selected parameters can lead to lower cost for a thermal-neural biorefinery.

INTRODUCTION

Fossil-based fuels and chemicals have provided the majority of energy needed for human development over the last century (U.S. Energy Information Administration, 2018). However, with the rising concerns over global warming and depleting fossil resources, the global community has come to the conclusion that a switch to renewable sources is critical to sustain future developments (UNGA, 2015). In US, a potential biomass availability of more than 1 billion dry tons per year is projected by 2030 providing a large resource for renewable energy (Langholtz et al., 2016). Lignocellulosic biomass is of particular interest as it can be collected in large quantities from agricultural and forestry resources and is inedible and carbon neutral, avoiding food vs fuel issues associated with grain and crop based biomass (Sun et al., 2018).

Lignocellulosic biomass has three major constituents: cellulose, hemicellulose, and lignin (Mussatto, 2016). Cellulose (30–50 wt%) is a linear chain polysaccharide consisting of hundreds to thousands of β (1→4)-linked D-glucose molecules (Upton and Kasko, 2016). Hemicellulose (20–35 wt%) is an amorphous heteropolymer of primarily xylose sugars (Gibson, 2012). Lignin (15–30 wt%) is a complex aromatic heteropolymer derived from three cinnamyl alcohol monomers, i.e., p-coumaryl alcohol, coniferyl alcohol, and sinapyl alcohol linked by carbon-carbon and ether bonds producing, respectively, p-hydroxyphenyl (H), guaiacyl (G), and syringyl phenylpropanoid (S) units in lignin polymer (Boerjan et al., 2003; Ralph et al., 2019). To develop economical and sustainable biorefineries, all three major constituents must be effectively converted to value-added products. Over the last decades, significant progress has been made in cellulose and hemicellulose deconstruction and monomer upgrading technologies to fuels and chemicals (Chandel et al., 2018; Langan et al., 2011; Op de Beeck et al., 2015; Peng et al., 2012; Zabed et al., 2016). In contrast, lignin valorization technologies have been limited, for the most part, to heat and power production (Da Costa Sousa et al., 2016; Vardon et al., 2015).

Native lignin is covalently cross-linked with hemicellulose, which together form an amorphous structure to enclose and protect cellulose fibers from microbial attack (Schutyser et al., 2018). Biomass deconstruction is performed to breakdown the covalent bonds with holocellulose (cellulose and hemicellulose) and yield isolated lignin prior to valorization. Generally, fractionation strategies can be divided into two categories: (1) methods resulting in lignin release from the biomass called delignification and (2) methods targeting conversion and solubilization of carbohydrates. Delignification processes include alkaline, acidic, reductive, ionic liquid dissolution, and mechanical pretreatment followed by extraction, which produce lignin precipitate or depolymerized lignin oil. The second category includes acid-catalyzed hydrolysis, enzyme-assisted hydrolysis, and thermal processes, which isolate lignin in the form of precipitate or insoluble residue. See Schutyser et al. (Schutyser et al., 2018) for a detailed review of each category.

[1]Department of Chemical and Biological Engineering and DOE Great Lakes Bioenergy Research Center, University of Wisconsin-Madison, 1415 Engineering Drive, Madison, WI 53706, USA

[2]Lead Contact

*Correspondence: christos.maravelias@wisc.edu

https://doi.org/10.1016/j.isci.2019.100751

Native lignin polymer contains carbon-carbon and ether inter-unit connections (Boerjan et al., 2003; Vanholme et al., 2010). The most abundant linkage bond (>50%) is β-O-4 alkyl-aryl ether linkage, which, along with α-O-4 ether linkage, is the most easily cleavable bond (Chakar and Ragauskas, 2004). Considering that carbon-carbon bonds are difficult to break, the majority of lignin depolymerization strategies target the ether bonds (Gall et al., 2017; Rahimi et al., 2014). Generally, the theoretical monomer yield is proportional to the square of the relative content of inter-unit ether bonds (Yan et al., 2008). Therefore, to achieve higher depolymerization yields, the ether bonds must remain intact during biomass fractionation. The monomer yield from lignin strongly depends on three major factors: (1) isolation strategy, (2) depolymerization strategy, and (3) lignin origin (biomass type) (Schutyser et al., 2018). Lignin depolymerization strategies could be categorized to (1) reductive, (2) oxidative, (3) base- and acid-catalyzed, (4) solvolytic and thermal, and (5) two-step depolymerization (Schutyser et al., 2018). Table 1 provides a summary of each category. For a more detailed discussion, readers are referred to reviews of this topic (Behling et al., 2016; Li et al., 2015; Ma et al., 2015; Mu et al., 2013; Schutyser et al., 2018; Xiu and Shahbazi, 2012; Zakzeski et al., 2010).

Some of the lignin depolymerization monomers such as vanillin can be sold without further transformation. However, many other monomer streams require additional processing to narrow the wide range of monomers into targeted categories to (1) favor economical separation and recovery and (2) produce marketable products. Generally, monomer upgrading can be accomplished through biocatalytic or chemocatalytic processes.

In biocatalytic processes, depolymerized lignin is transformed to value-added chemicals mostly using aerobic microbial organisms (Schutyser et al., 2018). Microorganisms could be genetically engineered to defunctionalize aromatic compounds into intermediate products such as gallate, protocatechuate, and catechol. Dioxygenase enzymes could further ring-open the intermediate products and utilize them in central carbon metabolism (Abdelaziz et al., 2016; Masai et al., 2007, 2012). Metabolic engineering has enabled the use of microorganisms for the production of chemicals such as vanillin (Varman et al., 2016), medium-chain-length polyhydroxyalkanoates (Linger et al., 2014), muconic acid (Vardon et al., 2015), pyridine dicarboxylic acids (Mycroft et al., 2015; Perez et al., 2019), and fatty acids (Zhao et al., 2016), which could be further upgraded to high-value chemicals and polymer building blocks.

Chemocatalytic upgrading reactions can be divided into two categories: (1) reactions that transform phenolic core and its substitution degree and (2) reactions that target structure of side-chains (Schutyser et al., 2018). In phenolic core transformation, defunctionalization of core phenol is targeted using hydrodeoxygenation (HDO) reactions to reduce the complexity, functionality, H/C, and O/C ratio in depolymerization products. Accordingly, the HDO reactions could target production of four types of products: (1) alkenes, (2) aromatics, (3) phenols, and (4) cyclohexanols, which are different in oxygen content (depending on partial or complete HDO) and aromaticity (ring hydrogenation or preservation). Table 2 provides a summary of characteristics and operating conditions of monomer upgrading processes. More detailed reviews of upgrading processes are available in the literature (Abdelaziz et al., 2016; Beckham et al., 2016; Bugg and Rahmanpour, 2015; Laskar et al., 2013; Li et al., 2015; Zakzeski et al., 2010).

In summary, lignin is the second most abundant natural polymer accounting for about 30% of organic carbon in the biosphere and is the largest renewable source of aromatic monomers (Li et al., 2018; Stolark, 2017). The polyphenolic structure of lignin can potentially be used to produce value-added chemicals, functional materials, and fuel products (Schutyser et al., 2018; Zhang et al., 2017). However, being at early stage of development, the economic viability of lignin valorization strategies and their integration within biorefineries are not known.

Accordingly, the goal of this paper is to study what technological advances are necessary for lignin valorization technologies to become attractive or, equivalently, what is the impact of uncertainty in some key lignin-valorization-related technological and economic parameters on the viability of lignin valorization strategies. Toward this goal, we first generate a superstructure to represent potential biorefinery configurations (Figure 1) and then a mixed-integer nonlinear programming model (see Methods for details) to identify the optimal process to achieve specific objectives while satisfying given constraints. Using this optimization model, we then evaluate the impact of four critical lignin valorization parameters on the energy efficiency and economics: (1) energy requirement of conversion, (2) conversion efficiency to bioproducts, (3) production cost, and (4) market value of bioproducts.

Depolymerization	Catalyst	Additives	Solvents	T (°C)	P_{H2} (bar)	Selectivity	Yield
Reductive							
Mild hydroprocessing (MHD)	Nobel metal, base metal, mixed metal	H_3PO_4, HCl, MCl_x, NaOH, KOH, Na_2CO_3	H_2O, MeOH, EtOH, iPrOH, dioxane, tetrahydrofuran, or solvent mixture	130–390	10–100	High toward methoxyphenols or catechols	Moderate <20wt%
Harsh hydroprocessing (HHD)	Nobel metal, base metal		Mostly solventless, MeOH, 1-methylnaphthalene	320–450	35–100	Low toward phenol, methylated phenols, and phenols with long alkyl chains	Moderate <30wt%
Bifunctional hydroprocessing (BHD)	Nobel metal, base metal		H_2O, MeOH, tetrahydrofuran, heptane, methyl cyclohexane, dodecane, hexadecane	150–320	20–70	High toward cycloalkanes C_6–C_{18}	High <50%–70%
Liquid phase reforming (LPRD)	Nobel metal, base metal	H-zeolites, nafion SAC-13, H_3PO_4, heteropolyacid, NaOH	H_2O, formic acid, MeOH, EtOH, iPrOH, tetralin, glycerol	150–400	Liquid phase	Very low toward a broad range of compounds	High 20%–86%

Depolymerization	Catalyst	Oxidants	Solvents	T (°C)	P_{O2} (bar)	Selectivity	Yield
Oxidative							
Alkaline oxidation to phenolics (AlOF)	Soluble catalyst, solid catalyst	O_2	NaOH in H_2O, MeOH, EtOH, dioxane, tetrahydrofuran, KOH in water	120–190	2–14	High toward phenolic aldehydes such as vanillin	Low <10%–20%
Acidic (AcOF) and pH-neutral (NOF) lignin oxidation to phenolics	Soluble catalyst, solid catalyst	O_2, H_2O_2, peracetic acid	H_2O, MeOH, acetic acid, methyl isobutyl ketone, ionic liquid	60–210	5–30	Moderate toward phenols	Low <10–20%
Lignin oxidation to non-phenolic carboxylic acids (OCA)	Solid catalyst	O_2, H_2O_2	Mainly liquid phase H_2O (neutral), acidic (H_2SO_4 or acetate buffer), alkaline (NaOH)	60–225 (liquid phase), 327–377 (gas phase)		High toward carboxylic acids (formic, acetic, succinic, oxalic, and malonic acids)	High 10%–60%

Depolymerization	Catalyst	Additives	Solvents	T (°C)	Selectivity	Yield
Base- & Acid-Catalyzed						
Base-catalyzed depolymerization (BCD)	Soluble base (mostly NaOH) or solid base		H_2O (mostly), MeOH, EtOH, iPrOH, tetrahydrofuran, 3-methyl-3-pentanol	240–330	Moderate, methoxyphenols (T < 300), catechol (T > 300)	<10%–20%
Acid-catalyzed depolymerization (ACD)	Lewis acid, solid or soluble Brønsted acid	$[Ir(cod)Cl]_2/PPh_3$, $[Rh(cod)Cl]_2$/dppp	H_2O, MeOH, EtOH, iPrOH, 1-BuOH, ethylene glycol, dioxane, octane, formic acid	140–400	Low with wide array of products, methoxyphenols (T < 300), catechol (T > 300)	<20%–60%

Depolymerization	Catalyst	Solvents	T (°C)	Selectivity	Yield	Note
Solvolytic & Thermal						
Solvolytic (SLD)		Water, MeOH, EtOH, iPrOH, 1-BuOH, tetrahydrofuran, acetone, octane, dihydroanthracene, tetralin, naphthalene, solvent mixture	250–450	Low	<10%–20%	Hydrogen-donating solvents are mostly used

Table 1. Summary and Characteristics of Lignin Depolymerization Strategies

(Continued on next page)

Depolymerization	Catalyst	Solvents	T (°C)	Selectivity	Yield	Note
Fast pyrolysis (FPD)			400–800	Low	<20%	Under inert atmosphere
Catalytic fast pyrolysis (CFP)	*In situ* or *ex situ*: silica/alumina, zeolites, metal on zeolite oxides		500–700	High toward deoxygenated aromatics, benzene, toluene, xylene, and naphthalene	<30%	Under inert atmosphere

Depolymerization	Catalyst 1st Stage	Catalyst 2nd Stage	T (°C)	Selectivity	Yield	Note
Two-Stage						
Benzylic alcohol oxidation and depolymerization (BAOD)	4-acetoamide-TEMPO/HNO_3/HCl, DDQ/tBuONO, [4-AcNH-TEMPO]BF_4-mediated, NHPI/2,6-lutidine-mediated	Aqueous formic acid/sodium formate	110	Phenolic diketones (syringyl- and guaiacyl-1,2-propanedione), aldehydes (syringaldehyde and vanillin), and acids (syringic, vanillic, and p-hydroxybenzoic acid)	52%	Under aerobic oxidation or electrocatalytic oxidation
Benzylic alcohol methylation and depolymerization (BAMD)	$Al_2(SO_4)_3$	Pd/C, liquid phase reforming in methanol/formic acid	280	Low	17%	Under microwave radiation and methanol solvent

Table 1. Continued

Based on our literature review, we determine base values for the parameters describing the lignin depolymerization, monomer upgrading, and bioproduct separation process, defined collectively as the lignin valorization (LV) block. However, to keep the analysis general and given the scarcity of detailed techno-economic analysis (TEA) studies for lignin-based chemical production, we do not specify the target bioproducts and conversion and separation technologies used in the LV block. Rather, we establish targets in terms of the four key parameters, thereby providing insights into critical areas of improvement for viable lignin valorization. We do so for strategies considering both depolymerization (Table 1) and monomer upgrading (Table 2).

RESULTS AND DISCUSSION

Base Case

The material and energy balances for the optimal strategy under the base case parameters (see Tables S1–S3 for the base values of the parameters describing each block) are shown in Figure 2. Note that this strategy is the same as the base case strategy (S^{BC}) reported by Ng et al. (2019), in which lignin valorization (LV block) is not selected. S^{BC} includes GVL, COFER2, SEP2, WWT, CB, and TBG1 blocks and has a minimum cost of \$0.76/kg ethanol, which is equivalent to a minimum ethanol selling price (MESP) of \$3.44/GGE. If we enforce the selection of lignin valorization by fixing the binary variable for the LV block ($Y_{LV} = 1$), the lignin stream from the GVL block will be split, and a fraction of it will be sent to LV satisfying the lower bound on production level. Thus, the optimal solution in this case, referred to as $S^{BC\text{-}LV}$ (see Figure 2), will depend on the selected lower capacity (e.g., $\underline{\zeta}_{LV} = 0.039$).

In the reminder of the paper, we study how changes in four key parameters for LV alter the optimal design, economics, and energy efficiency of a lignocellulosic biorefinery. In other words, we study how uncertainty in these parameters impact the optimal biorefinery configuration and its key performance metrics. Before we present the detailed results, we note that a number of other parameters are stochastic. However, although the impact of uncertainty in these parameters on the minimum ethanol cost can be significant (see Figure S4), the major insights of this study, in terms of technological targets, remain the same (see discussion in Transparent Methods). This is because these other parameters impact both the lignin-to-heat/power and lignin-to-bioproducts strategies. For example, an increase in feedstock price will lead to a more *expensive* lignin stream, but the fundamental trade-off we study (lignin-to-heat/power vs. lignin

Upgrading Process	Target Products	Product Value	C-H-O Ratio	Catalyst	Note
Chemocatalytic	Alkanes and cyclohexanes	Low-value, mid-range fuel additive	High H/C, low O/C	Noble metals (Ru, Rh, Pd, Pt), Ni-based catalyst, H_3PO_4, acetic acid, acidic IL, HZSM-5, HBEA	Monomers are ring opened and products are fully deoxygenated
	Aromatic hydrocarbons	Low value, mid-range fuel additive	Low H/C, low O/C	Co-Mo, NiMo, MoO_3, FeMoP, Ru/TiO_2, PdFe/C, PtCo/C	Operated at gas phase, high temperature, and low H_2 pressure (<1 bar) for CO hydrogenation. Products are fully deoxygenated
	Cyclohexanols	As feed for synthesis of high-value monomers (e.g., adipic acid and polyester building blocks)	High H/C, high O/C	Ni/CeO_2, Ni/SiO_2–Al_2O_3, RANEYs Ni, CoN_x/C,Ru/ZrO_2–$La(OH)_3$, Ru–MnO_x/C, and Ru/C + MgO	Operated in liquid phase, partial HDO, demethoxylation, and aromatic ring hydrogenation
	Phenols	As feed for synthesis of high-value monomers (e.g., terephthalic acid, ethylene, propylene, and phenol)	Low H/C, high O/C	Nobel metal, base metal,	Selective demethoxylation
Biological	Vanillin, medium-chain-length polyhydroxyalkanoates, muconic acid	Precursor to adipic acid, terephthalic acid, pyridine dicarboxylic acids, and fatty acids			Close to theoretical yields obtained from representative components such as p-coumarate, ferulate, and benzoate

Table 2. Summary and Characteristics of Upgrading Strategies for Lignin-Derived Monomers

valorization) will not be noticeably impacted. Thus, although the minimum ethanol cost may change, the trends and the parameter values of the LV block at which strategy transitions occur will remain practically the same.

Analysis

To identify the major drivers for lignin valorization, we study the impact of the following parameters on the optimal biorefinery configuration and minimum ethanol cost: (1) conversion coefficient, (2) unit conversion cost, (3) bioproduct selling price, and (4) energy requirement. The first two depend on the efficiency of both conversion and separation technology employed within the valorization block, whereas the third one depends on the selected bioproduct. Additionally, the energy requirement depends on the energy input necessary for conversion (e.g., heat) and separation (e.g, heat and power). We note that, from a sustainability standpoint, a thermal-neutral biorefinery is always favorable, especially for biofuel, as opposed to biochemical, production (Humbird et al., 2011). Here, the term "thermal-neutral" refers to a biorefinery that is energetically self-sufficient through byproduct stream burning (e.g., unconverted lignin, biogas from anaerobic digestion, and biomass sludge from WWT) to generate steam and electricity and additional revenue through excess electricity sale (Humbird et al., 2011).

Conversion Coefficient and Bioproduct Selling Price

First, the sensitivity of the minimum ethanol cost is evaluated with respect to conversion coefficient and bioproduct selling price at a fixed unit conversion cost ($0.16/kg-lignin) and energy requirement (2.7 kWh/kg-lignin of heat and 0.05 kWh/kg-lignin of electricity) for the LV block. The results of this analysis are shown in Figure 3A. The minimum ethanol cost decreases with the increase of conversion coefficient and bioproduct selling price if the LV block is selected. In contrast, the minimum ethanol cost remains the same for the S^{BC} strategy at the bottom left region (region on the left of the white dashed line), which is selected when the conversion coefficient and bioproduct selling price are low.

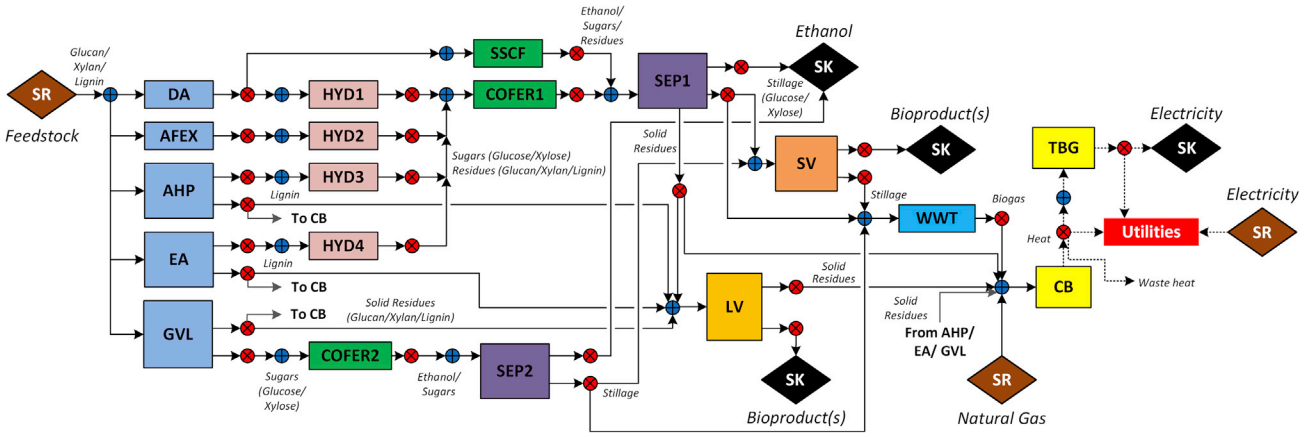

Figure 1. Corn Stover-to-Ethanol Superstructure

Abbreviations—AFEX: ammonia fiber expansion, AHP: copper-catalyzed alkaline hydrogen peroxide, CB: combustor and boiler, COFER: co-fermentation, DA: dilute acid, EA: extractive ammonia, GVL: γ-valerolactone, HYD: hydrolysis, LV: lignin valorization, SEP: separation, SSCF: simultaneous saccharification and co-fermentation, SV: stillage valorization, TBG: turbogenerator, WWT: wastewater treatment.

Figure 3 can also be used to predict the economic feasibility of a lignin valorization technology. For example, if a technology is developed to further convert intermediate bioproducts (e.g., monomers) to a high-value chemical via monomer upgrading (e.g., see strategies listed in Table 2), the selling price of the chemical should be at least \$1.3/kg if 80% yield is achieved for this additional step (0.24 overall conversion coefficient).

We also observe that the optimal pretreatment technology switches from GVL to AFEX at the top right region, above the gray dashed line, if both conversion coefficient (>0.43 kg-bioproduct/kg-lignin) and bioproduct selling price (>\$2.6/kg) are high. Figure 4 shows the optimal strategies with the GVL block and AFEX block, respectively, based on the same conversion coefficient (0.48 kg-bioproduct/kg-lignin) and bioproduct selling price (\$2.8/kg). The optimal strategy with the AFEX block has a higher product yield but also higher energy requirement than the one with the GVL block. To illustrate the trade off, we plot the minimum ethanol cost as a function of bioproduct price with fixed conversion coefficient for the two strategies (see Figure 5). Although the minimum ethanol cost of both strategies decreases with the bioproduct selling price, a higher product yield (0.362 kg-bioproduct/kg-ethanol vs 0.284 kg-bioproduct/kg-ethanol) leads to a faster reduction and it offsets the exceeded production cost when the bioproduct price goes beyond \$2.73/kg.

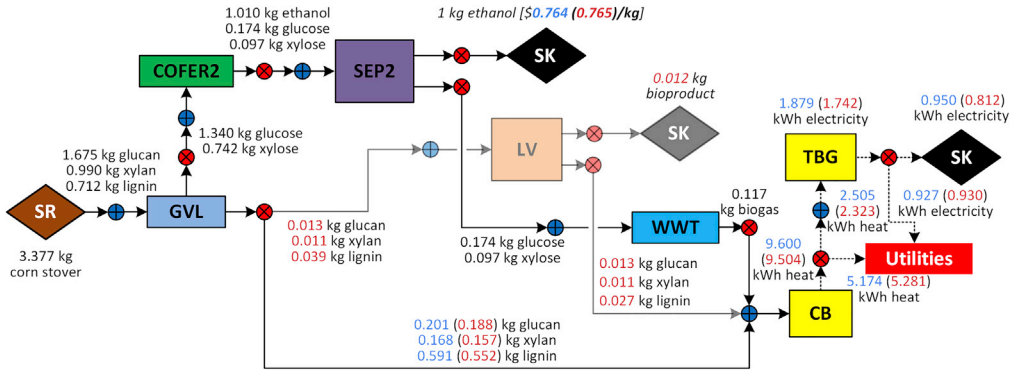

Figure 2. Strategies S^{BC} (GVL-COFER2-SEP2-WWT-CB-TBG1) and $S^{BC\text{-}LV}$ (GVL-COFER2-SEP2-LV-WWT-CB-TBG1)

The faded arcs that are connected to the LV block are only applicable to the $S^{BC\text{-}LV}$ strategy. Black fonts before the SEP2 block are identical for both S^{BC} and $S^{BC\text{-}LV}$ strategies, whereas blue and red fonts after the SEP2 block represent the flows related to S^{BC} and $S^{BC\text{-}LV}$ strategies, respectively.

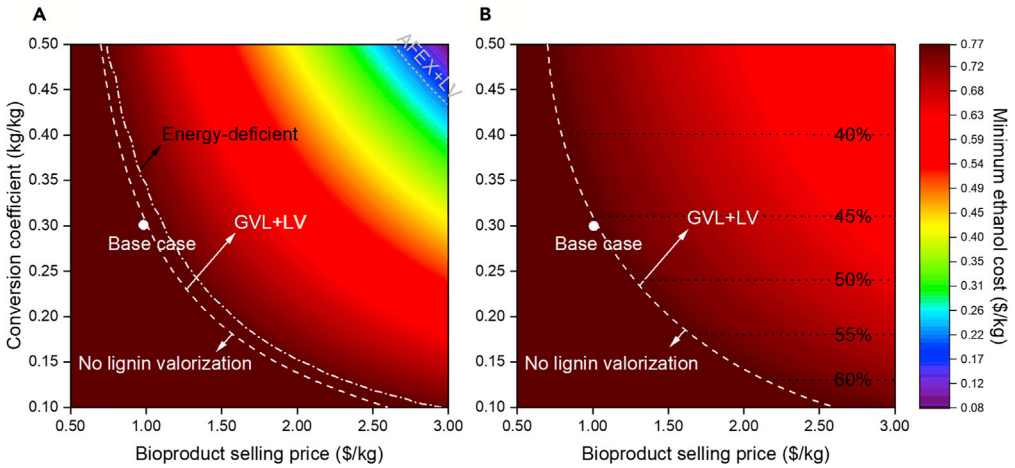

Figure 3. Minimum Ethanol Cost as a Function of Conversion Coefficient and Bioproduct Selling Price for the LV Block

(A) optimal solutions, based on economic metric, and (B) solutions that achieve a thermal-neutral biorefinery. White circle points indicate base case parameters; white dashed lines represent configuration transitions; gray dashed line represents pretreatment technology transition; white dash-dotted line represents thermal-neutral transition; black dotted lines represent lignin utilization percentage in the LV block.

The optimal strategies with lignin valorization tend to be energetically deficient because the generated energy from the remaining lignin is not sufficient to meet biorefinery demand (see region above and to the right of the white dashed dot line in Figure 3A). When LV is selected, natural gas and/or electricity is purchased because revenue from bioproducts sales is higher than the cost of purchased energy. Thus, we next consider strategies subject to the constraint that neither natural gas nor electricity is purchased. The strategy with the AFEX block is no longer selected (see Figure 3B) because it requires more energy than the one with the GVL block. Unlike the strategies leading to the results in Figure 3A, the optimal strategies with the LV block do not fully valorize lignin. Instead, a fraction of lignin is used for heat and power generation; the split ratio is determined by the conversion coefficient of the LV block. For example, 50% of lignin is used to produce bioproduct if the conversion coefficient is 0.24 and bioproduct selling price is greater than $1.2/kg. When the conversion coefficient increases, the utilization of lignin in the LV block decreases. Overall, when energy-related constraints are added, the optimal strategies with the LV block have higher minimum ethanol cost than those in Figure 3A. Because a thermal-neutral biorefinery is preferred, the following analysis focuses on the strategies with no externally purchased natural gas and/or electricity.

Production Cost and Bioproduct Selling Price

Here, for the LV block, we define the production cost ($/kg-bioproduct) as the quotient of the unit conversion cost ($/kg-lignin) by the conversion coefficient (kg-bioproduct/kg-lignin). This allows us to study the minimum ethanol cost as a function of the bioproduct selling price and production cost at a fixed conversion coefficient ($0.3 kg-bioproduct/kg-lignin) by changing its unit conversion cost. Clearly, higher bioproduct selling price and lower production cost lead to lower minimum ethanol cost. Because the conversion coefficient is fixed, the fraction of valorized lignin is 45%, whereas the remaining lignin is sent for heat and power generation. Similar to Figure 3B, the GVL block is preferred for pretreatment along with the LV block when the biorefinery is thermal-neutral.

Alternatively, we can plot the minimum ethanol cost in terms of the bioproduct selling price and production cost, considering a unit conversion cost equal to $0.162/kg-lignin but changing the conversion coefficient (see Figure 6B). Parameter combinations below and to the right of the white dashed line lead to lower minimum ethanol cost than those in Figure 6A. This indicates that conversion coefficient improvements are preferred over unit conversion cost reductions for the same production cost because an increase in bioproduct production leads to more revenue. Also, we see that the lignin utilization ratio is correlated with the conversion coefficient if the LV block is selected. For example, in Figure 6B, 50% lignin utilization

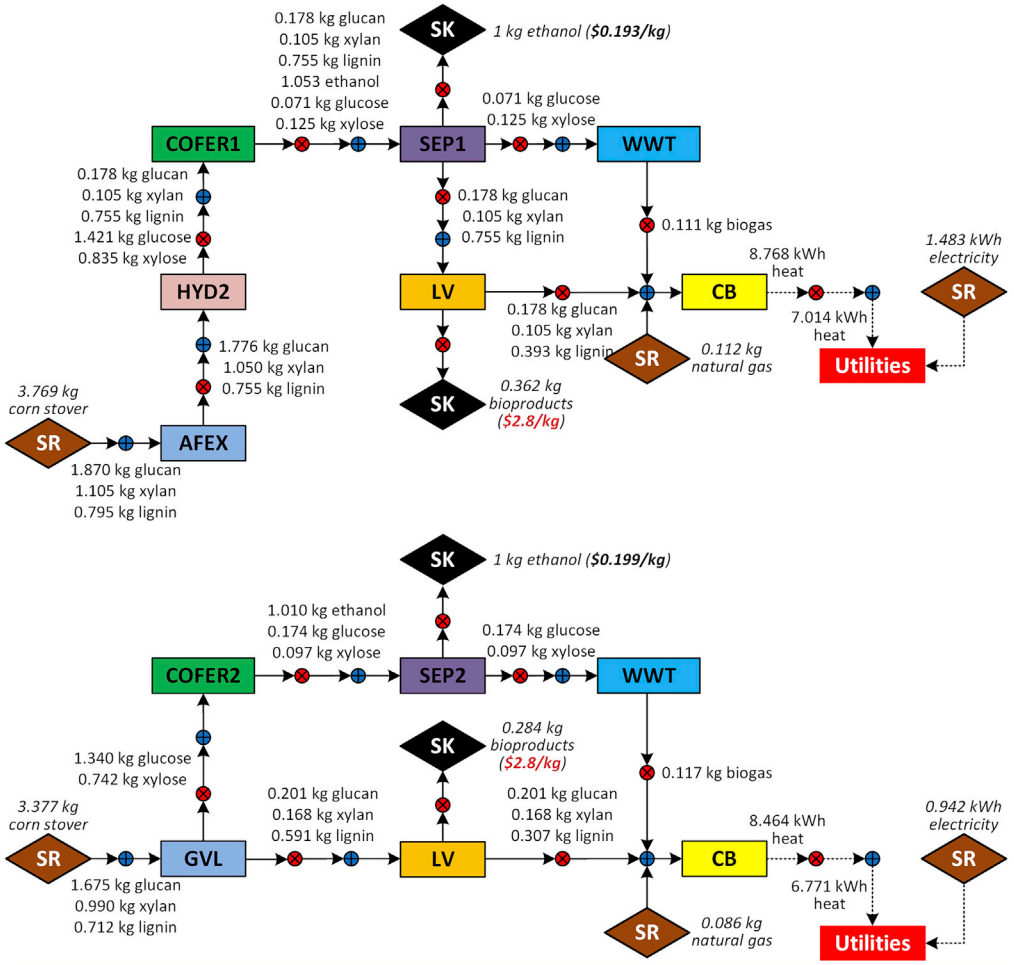

Figure 4. Optimal Configurations with the GVL Block and AFEX Block Using Same Conversion Coefficient (0.48 kg-Bioproduct/kg-Lignin) and Bioproduct Selling Price ($2.8/kg)

corresponds to a production cost of $0.675/kg-bioproduct, which is equivalent to 0.24 kg-bioproduct/kg-lignin conversion coefficient when the unit conversion cost is fixed at $0.162/kg-lignin. This is consistent with the correlation between conversion coefficient and lignin utilization in Figure 6B.

Profit and Energy Requirement

To understand the trade-offs between the economic and energy-related drivers, we combine all parameters considered in the previous sections in one parameter (called "profit") and study its impact, along with the impact of energy requirement (kWh/kg-bioproduct), on the minimum ethanol cost. The profit ($/kg-bioproduct) for the LV block is calculated by

$$\text{Profit}(\$/\text{kg-bioproduct}) = \text{Bioproduct selling price } (\$/\text{kg}) - \frac{\text{Conversion cost } (\$/\text{kg-lignin})}{\text{Conversion coefficient } (\text{kg-bioproduct}/\text{kg-lignin})}$$

For illustration, we change the profit by varying the bioproduct selling price from $0.5–3.0/kg while keeping the other parameters at their base case values. The results are shown in Figure 7. No lignin valorization is selected when the combination of profit and energy requirement is on the left of the white dashed line. Furthermore, since the conversion coefficient is fixed, the lignin utilization percentage of the LV block is now correlated with its energy requirement. A higher energy requirement leads to a lower ratio of lignin valorized to bioproduct because more lignin would be required to fulfill the energy demand for a thermal-neutral biorefinery.

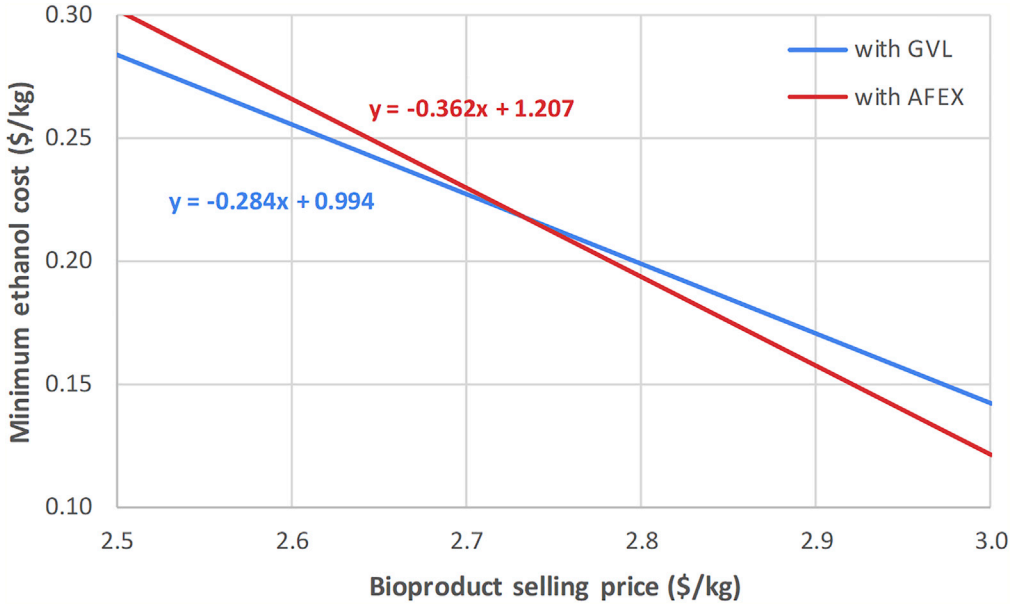

Figure 5. Minimum Ethanol Cost as a Function of Bioproduct Price with Fixed Conversion Coefficient

Conclusion

In this paper, we studied biorefinery strategies for the conversion of biomass to ethanol coupled with lignin valorization subsystems. Based on process synthesis through superstructure optimization, thousands of optimizations were performed to evaluate the impact of various parameters related to lignin valorization on the optimal biorefinery configuration and minimum ethanol cost. Interestingly, we showed that different pretreatment technologies may be selected under different constraints. Our analysis provided baseline results and suggested what advances can make lignin valorization economically attractive. We hope that our results coupled with the identification of appropriate lignin-derived products and development of economical separation technologies for bioproduct recovery will help accelerate the development of lignin valorization technologies.

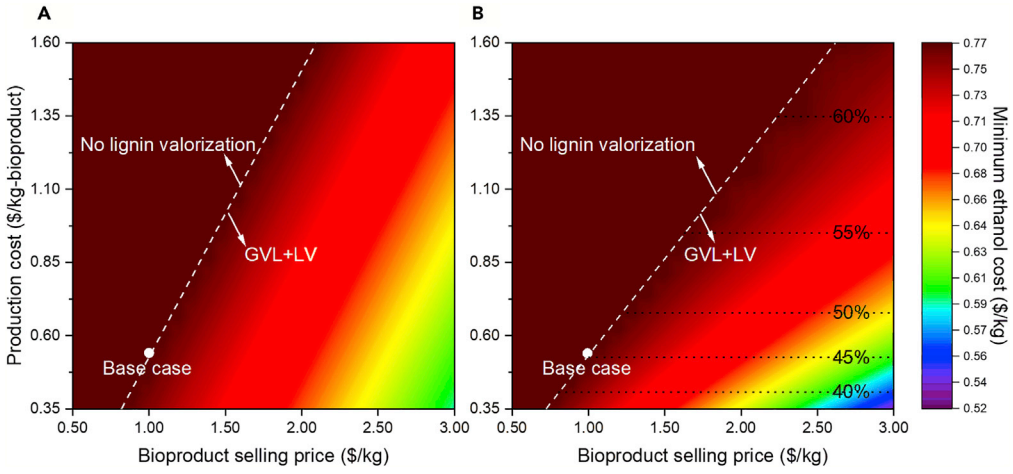

Figure 6. Minimum Ethanol Cost as a Function of Production Cost and Bioproduct Selling Price for the LV Block

Cost calculated by changing (A) unit conversion cost and fixing conversion coefficient at 0.3 kg-bioproduct/kg-lignin and (B) conversion coefficient and fixing unit conversion cost at $0.162/kg-lignin. White circle points indicate the base case parameters; white dash lines represent economic feasibility transitions; black dot lines represent lignin utilization percentage in the LV block.

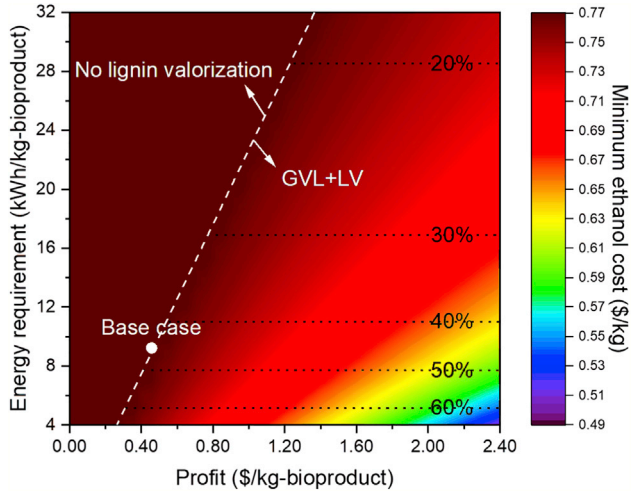

Figure 7. Minimum Ethanol Cost as a Function of Profit and Energy Requirement in the LV Block

White circle points indicate the base case parameters; white dash line represents economic feasibility transitions; black dot lines represent lignin utilization percentage in the LV block.

Limitations of the Study

Our goal is to identify general insights, and thus detailed analysis for specific lignin valorization products or strategies was not performed. However, detailed techno-economic analysis, including an assessment of the impact of uncertainty in key parameters (describing blocks other than LV), would become necessary when specific compounds and a detailed production process, including viable separation and recovery blocks, are identified.

METHODS

All methods can be found in the accompanying Transparent Methods supplemental file.

SUPPLEMENTAL INFORMATION

Supplemental Information can be found online at https://doi.org/10.1016/j.isci.2019.100751.

ACKNOWLEDGMENTS

This material is based upon work supported by the Great Lakes Bioenergy Research Center, U.S. Department of Energy, Office of Science, and Office of Biological and Environmental Research under Award Number DE-SC0018409.

AUTHOR CONTRIBUTIONS

Conceptualization, C.T.M., K.H., and P.F.; Methodology, K.H., C.T.M., and P.F.; Software, K.H.; Formal Analysis, K.H.; Investigation, K.H., P.F., and C.T.M.; Resources, K.H., P.F., and C.T.M.; Writing—Original Draft, K.H. and P.F.; Writing—Review & Editing, K.H., P.F., and C.T.M.; Visualization, K.H. and C.T.M.; Supervision, C.T.M.; Funding Acquisition, C.T.M.

DECLARATION OF INTERESTS

The authors declare no competing interests.

Received: July 26, 2019
Revised: October 15, 2019
Accepted: November 23, 2019
Published: January 24, 2020

REFERENCES

Abdelaziz, O.Y., Brink, D.P., Prothmann, J., Ravi, K., Sun, M., García-Hidalgo, J., Sandahl, M., Hulteberg, C.P., Turner, C., Lidén, G., and Gorwa-Grauslund, M.F. (2016). Biological valorization of low molecular weight lignin. Biotechnol. Adv. *34*, 1318–1346.

Beckham, G.T., Johnson, C.W., Karp, E.M., Salvachúa, D., and Vardon, D.R. (2016). Opportunities and challenges in biological lignin valorization. Curr. Opin. Biotechnol. *42*, 40–53.

Behling, R., Valange, S., and Chatel, G. (2016). Heterogeneous catalytic oxidation for lignin valorization into valuable chemicals: what results? What limitations? What trends? Green Chem. *18*, 1839–1854.

Boerjan, W., Ralph, J., and Baucher, M. (2003). Lignin biosynthesis. Annu. Rev. Plant Biol. *54*, 519–546.

Bugg, T.D., and Rahmanpour, R. (2015). Enzymatic conversion of lignin into renewable chemicals. Curr. Opin. Chem. Biol. *29*, 10–17.

Chakar, F.S., and Ragauskas, A.J. (2004). Review of current and future softwood kraft lignin process chemistry. Ind. Crops Prod. *20*, 131–141.

Chandel, A.K., Antunes, F.A.F., Terán-Hilares, R., Cota, J., Ellilä, S., Silveira, M.H.L., dos Santos, J.C., and da Silva, S.S. (2018). Bioconversion of hemicellulose into ethanol and value-added products. In Advances in Sugarcane Biorefinery, A.K. Chandel and M.H.L. Silveira, eds. (Elsevier), pp. 97–134.

Da Costa Sousa, L., Jin, M., Chundawat, S.P.S., Bokade, V., Tang, X., Azarpira, A., Lu, F., Avci, U., Humpula, J., Uppugundla, N., et al. (2016). Next-generation ammonia pretreatment enhances cellulosic biofuel production. Energy Environ. Sci. *9*, 1215–1223.

Gall, D.L., Ralph, J., Donohue, T.J., and Noguera, D.R. (2017). Biochemical transformation of lignin for deriving valued commodities from lignocellulose. Curr. Opin. Biotechnol. https://doi.org/10.1016/j.copbio.2017.02.015.

Gibson, L.J. (2012). The hierarchical structure and mechanics of plant materials. J. R. Soc. Interface *9*, 2749–2766.

Humbird, D., Davis, R., Tao, L., Kinchin, C., Hsu, D., Aden, A., Schoen, P., Lukas, J., Olthof, B., Worley, M., et al. (2011). Process Design and Economics for Biochemical Conversion of Lignocellulosic Biomass to Ethanol: Dilute-Acid Pretreatment and Enzymatic Hydrolysis of Corn Stover (National Renewable Energy Laboratory (NREL)). https://doi.org/10.2172/1013269.

Langan, P., Gnanakaran, S., Rector, K.D., Pawley, N., Fox, D.T., Cho, D.W., and Hammel, K.E. (2011). Exploring new strategies for cellulosic biofuels production. Energy Environ. Sci. *4*, 3820.

Langholtz, M.H., Stokes, B.J., and Eaton, L.M. (2016). 2016 Billion-Ton Report: Advancing Domestic Resources for a Thriving Bioeconomy (U.S. Department of Energy).

Laskar, D.D., Yang, B., Wang, H., and Lee, J. (2013). Pathways for biomass-derived lignin to hydrocarbon fuels. Biofuels, Bioprod. Biorefining *7*, 602–626.

Li, C., Zhao, X., Wang, A., Huber, G.W., and Zhang, T. (2015). Catalytic transformation of lignin for the production of chemicals and fuels. Chem. Rev. *115*, 11559–11624.

Li, Y., Shuai, L., Kim, H., Motagamwala, A.H., Mobley, J.K., Yue, F., Tobimatsu, Y., Havkin-Frenkel, D., Chen, F., Dixon, R.A., et al. (2018). An ideal lignin facilitates full biomass utilization. Sci. Adv. *4*, https://doi.org/10.1126/sciadv.aau2968.

Linger, J.G., Vardon, D.R., Guarnieri, M.T., Karp, E.M., Hunsinger, G.B., Franden, M.A., Johnson, C.W., Chupka, G., Strathmann, T.J., Pienkos, P.T., and Beckham, G.T. (2014). Lignin valorization through integrated biological funneling and chemical catalysis. Proc. Natl. Acad. Sci. U S A *111*, 12013–12018.

Ma, R., Xu, Y., and Zhang, X. (2015). Catalytic oxidation of biorefinery lignin to value-added chemicals to support sustainable biofuel production. ChemSusChem *8*, 24–51.

Masai, E., Katayama, Y., and Fukuda, M. (2007). Genetic and biochemical investigations on bacterial catabolic pathways for lignin-derived aromatic compounds. Biosci. Biotechnol. Biochem. *71*, 1–15.

Masai, E., Kamimura, N., Kasai, D., Oguchi, A., Ankai, A., Fukui, S., Takahashi, M., Yashiro, I., Sasaki, H., Harada, T., et al. (2012). Complete genome sequence of sphingobium sp. strain SYK-6, a degrader of lignin-derived biaryls and monoaryls. J. Bacteriol. *194*, 534–535.

Mu, W., Ben, H., Ragauskas, A., and Deng, Y. (2013). Lignin pyrolysis components and upgrading—technology review. BioEnergy Res. *6*, 1183–1204.

Mussatto, S.I. (2016). Biomass Fractionation Technologies for a Lignocellulosic Feedstock Based Biorefinery, Biomass Fractionation Technologies for a Lignocellulosic Feedstock Based Biorefinery (Elsevier). https://doi.org/10.1016/C2014-0-01890-4.

Mycroft, Z., Gomis, M., Mines, P., Law, P., and Bugg, T.D.H. (2015). Biocatalytic conversion of lignin to aromatic dicarboxylic acids in Rhodococcus jostii RHA1 by re-routing aromatic degradation pathways. Green Chem. *17*, 4974–4979.

Ng, R.T.L., Fasahati, P., Huang, K., and Maravelias, C.T. (2019). Utilizing stillage in the biorefinery: economic, technological and energetic analysis. Appl. Energy *241*, 491–503.

Op de Beeck, B., Dusselier, M., Geboers, J., Holsbeek, J., Morré, E., Oswald, S., Giebeler, L., and Sels, B.F. (2015). Direct catalytic conversion of cellulose to liquid straight-chain alkanes. Energy Environ. Sci. *8*, 230–240.

Peng, F., Peng, P., Xu, F., and Sun, R.C. (2012). Fractional purification and bioconversion of hemicelluloses. Biotechnol. Adv. https://doi.org/10.1016/j.biotechadv.2012.01.018.

Perez, J.M., Kontur, W.S., Alherech, M., Coplien, J., Karlen, S.D., Stahl, S.S., Donohue, T.J., and Noguera, D.R. (2019). Funneling aromatic products of chemically depolymerized lignin into 2-pyrone-4-6-dicarboxylic acid with: novosphingobium aromaticivorans. Green Chem. *21*, 1340–1350.

Rahimi, A., Ulbrich, A., Coon, J.J., and Stahl, S.S. (2014). Formic-acid-induced depolymerization of oxidized lignin to aromatics. Nature *515*, 249–252.

Ralph, J., Lapierre, C., and Boerjan, W. (2019). Lignin structure and its engineering. Curr. Opin. Biotechnol. https://doi.org/10.1016/j.copbio.2019.02.019.

Schutyser, W., Renders, T., Van den Bosch, S., Koelewijn, S.-F., Beckham, G.T., and Sels, B.F. (2018). Chemicals from lignin: an interplay of lignocellulose fractionation, depolymerisation, and upgrading. Chem. Soc. Rev. *47*, 852–908.

Stolark, J. (2017). If You Build it, They Will Come: Biofuels Industry Sees Renewable Chemicals as New Strategy [WWW Document] (Environmental and Energy Study Institute).

Sun, Z., Fridrich, B., de Santi, A., Elangovan, S., and Barta, K. (2018). Bright side of lignin depolymerization: toward new platform chemicals. Chem. Rev. *118*, 614–678.

U.S. Energy Information Administration. (2018). History of Energy Consumption in the United States, 1775–2009 [WWW Document] (Annual Energy Review 2009).

UNGA. (2015). Transforming Our World: The 2030 Agenda for Sustainable Development. In A New Era in Global Health (Springer Publishing Company).

Upton, B.M., and Kasko, A.M. (2016). Strategies for the conversion of lignin to high-value polymeric materials: review and perspective. Chem. Rev. *116*, 2275–2306.

Vanholme, R., Demedts, B., Morreel, K., Ralph, J., and Boerjan, W. (2010). Lignin biosynthesis and structure. Plant Physiol. *153*, 895–905.

Vardon, D.R., Franden, M.A., Johnson, C.W., Karp, E.M., Guarnieri, M.T., Linger, J.G., Salm, M.J., Strathmann, T.J., and Beckham, G.T. (2015). Adipic acid production from lignin. Energy Environ. Sci. *8*, 617–628.

Varman, A.M., He, L., Follenfant, R., Wu, W., Wemmer, S., Wrobel, S.A., Tang, Y.J., and Singh, S. (2016). Decoding how a soil bacterium extracts building blocks and metabolic energy from ligninolysis provides road map for lignin valorization. Proc. Natl. Acad. Sci. U S A *113*, E5802–E5811.

Xiu, S., and Shahbazi, A. (2012). Bio-oil production and upgrading research: a review. Renew. Sustain. Energy Rev. *16*, 4406–4414.

Yan, N., Zhao, C., Dyson, P.J., Wang, C., Liu, L., and Kou, Y. (2008). Selective degradation of wood lignin over noble-metal catalysts in a two-step process. ChemSusChem *1*, 626–629.

Zabed, H., Sahu, J.N., Boyce, A.N., and Faruq, G. (2016). Fuel ethanol production from lignocellulosic biomass: an overview on feedstocks and technological approaches. Renew. Sustain. Energy Rev. *66*, 751–774.

Zakzeski, J., Bruijnincx, P.C.A., Jongerius, A.L., and Weckhuysen, B.M. (2010). The catalytic valorization of lignin for the production of renewable chemicals. Chem. Rev. *110*, 3552–3599.

Zhang, Z., Song, J., and Han, B. (2017). Catalytic transformation of lignocellulose into chemicals and fuel products in ionic liquids. Chem. Rev. *117*, 6834–6880.

Zhao, C., Xie, S., Pu, Y., Zhang, R., Huang, F., Ragauskas, A.J., and Yuan, J.S. (2016). Synergistic enzymatic and microbial lignin conversion. Green Chem. *18*, 1306–1312.

ISCI, Volume *23*

Supplemental Information

System-Level Analysis of Lignin Valorization in Lignocellulosic Biorefineries

Kefeng Huang, Peyman Fasahati, and Christos T. Maravelias

Supplemental Figures

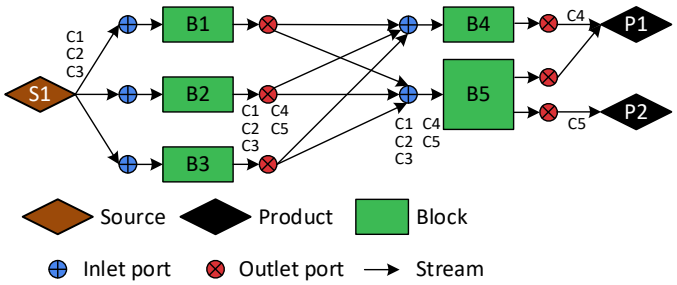

Figure S1. Representation of a general superstructure. B1 – B5 are blocks; C1 – C5 are components; SR1 and P1 – P2 are source and products, Related to **Figure 1**.

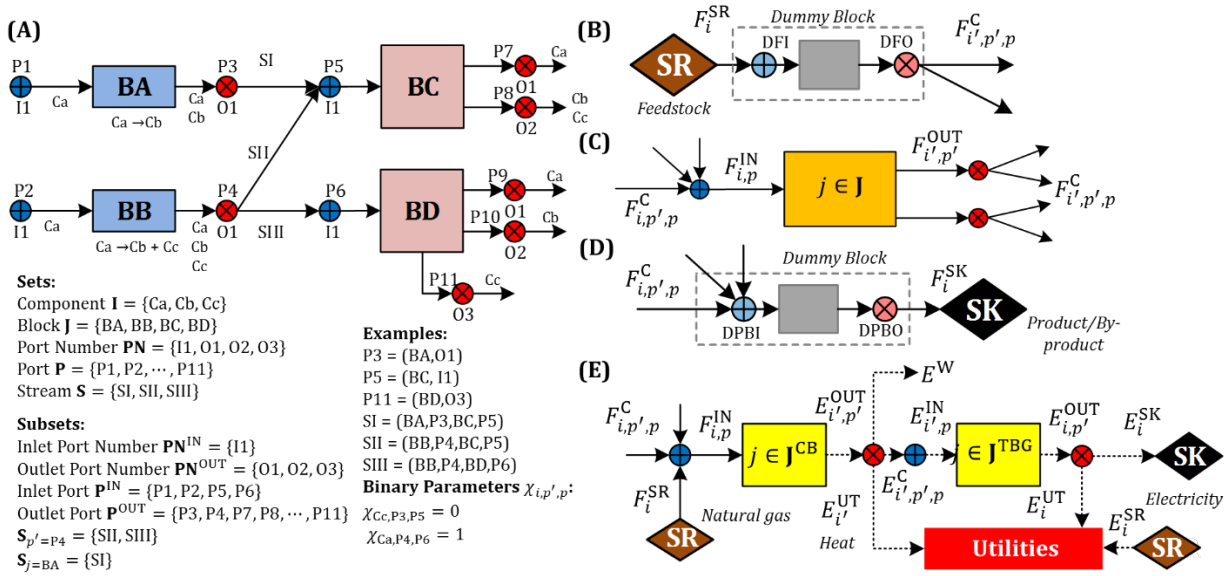

Figure S2. (A) Example of sets, subsets and binary parameters. (B) – (E) Generic mass and energy flow, Related to **Figure 1**.

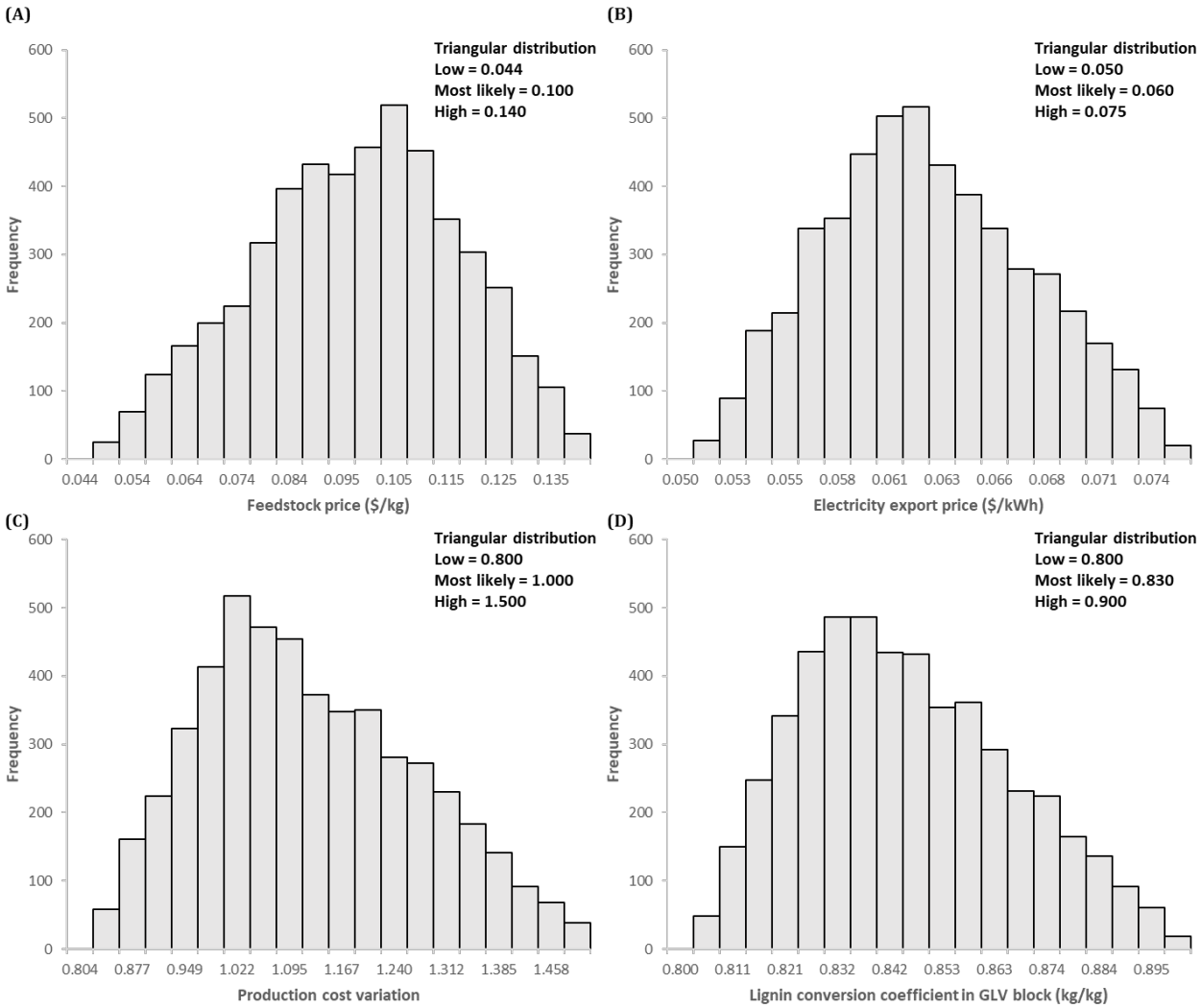

Figure S3. Histograms of values of parameters used for the assessment of the impact of uncertainty on the ethanol cost of the base case strategy. (A) Feedstock price, (B) Electricity export price, (C) Production cost variation, and (D) Lignin conversion coefficient in GVL block. Note that production cost variation is used as a multiplier to the sum of the production costs of all process blocks, Related to **Figure 2**.

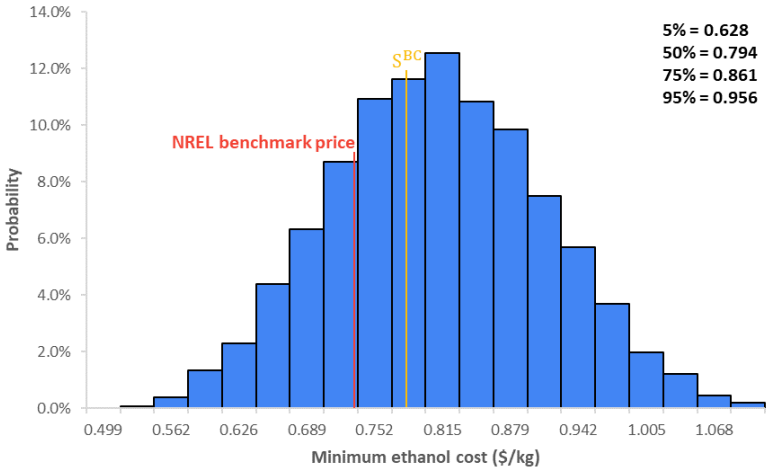

Figure S4. Distribution of the minimum ethanol cost of the base case in the scenarios generated by varying the values of four key parameters not directly related to lignin valorization (histograms of values shown in **Figure S3**), Related to **Figure 2**.

Supplemental Tables

Table S1. Composition of feedstock and unit price of components, Related to **Figure 1**.

Item	Value
Composition of Corn Stover	
Glucan	0.496
Xylan	0.293
Lignin	0.211
Unit Price λ_i ($ kg^{-1} or *$ kWh^{-1})	
Corn Stover	0.100
Natural Gas (purchase)	0.600
Electricity (export)	0.060*
Electricity (purchase)	0.065*
Bioproducts (SV)	2.000
Bioproducts (LV)	1.000

Table S2. Conversion coefficient of each block, Related to **Figure 1.**

i	i'	j	pn	pn	$\eta_{i,p,i',p'}$
Glucan	Glucose	DA	I1	O1	0.111
Glucan	Glucan	DA	I1	O1	0.900
Xylan	Xylose	DA	I1	O1	1.023
Xylan	Xylan	DA	I1	O1	0.100
Lignin	Lignin	DA	I1	O1	0.950
Glucan	Glucose	HYD1	I1	O1	1.000
Glucan	Glucan	HYD1	I1	O1	0.100
Xylan	Xylan	HYD1	I1	O1	1.000
Glucose	Glucose	HYD1	I1	O1	0.891
Xylose	Xylose	HYD1	I1	O1	0.871
Lignin	Lignin	HYD1	I1	O1	1.000
Glucose	Ethanol	COFER1	I1	O1	0.486
Xylose	Ethanol	COFER1	I1	O1	0.434
Glucose	Glucose	COFER1	I1	O1	0.050
Xylose	Xylose	COFER1	I1	O1	0.150
Glucan	Glucan	COFER1	I1	O1	0.990
Xylan	Xylan	COFER1	I1	O1	0.990
Lignin	Lignin	COFER1	I1	O1	1.000
Glucose	Ethanol	SSCF	I1	O1	0.350
Xylose	Ethanol	SSCF	I1	O1	0.330
Glucan	Ethanol	SSCF	I1	O1	0.510
Glucan	Glucose	SSCF	I1	O1	0.060
Xylose	Xylose	SSCF	I1	O1	0.150

Table S2 (continued)**.** Conversion coefficient of each block, Related to **Figure 1.**

i	i'	j	pn	pn	$\eta_{i,p,i',p'}$
Glucan	Glucan	SSCF	I1	O1	0.089
Xylan	Xylan	SSCF	I1	O1	0.990
Lignin	Lignin	SSCF	I1	O1	1.000
Ethanol	Ethanol	SEP1	I1	O1	0.950
Glucose	Glucose	SEP1	I1	O2	1.000
Xylose	Xylose	SEP1	I1	O2	1.000
Glucan	Glucan	SEP1	I1	O3	1.000
Xylan	Xylan	SEP1	I1	O3	1.000
Lignin	Lignin	SEP1	I1	O3	1.000
Glucose	Bioproducts (SV)	SV	I1	O1	0.300
Glucose	Glucose	SV	I1	O2	0.700
Xylose	Bioproducts (SV)	SV	I1	O1	0.300
Xylose	Xylose	SV	I1	O2	0.700
Glucose	Biogas	WWT	I1	O1	0.267
Xylose	Biogas	WWT	I1	O1	0.733
Biogas	Heat	CB	I1	O1	16.670
Glucan	Heat	CB	I1	O1	7.580
Xylan	Heat	CB	I1	O1	7.580
Lignin	Heat	CB	I1	O1	8.200
Lignin	Bioproducts (LV)	LV	I1	O1	0.300
Lignin	Lignin	LV	I1	O2	0.700
Glucan	Glucan	LV	I1	O2	1.000
Xylan	Xylan	LV	I1	O2	1.000
Glucan	Glucan	AFEX	I1	O1	0.950
Xylan	Xylan	AFEX	I1	O1	0.950
Lignin	Lignin	AFEX	I1	O1	0.950
Glucan	Glucose	HYD2	I1	O1	0.800
Glucan	Glucan	HYD2	I1	O1	0.100
Xylan	Xylan	HYD2	I1	O1	0.100
Xylan	Xylose	HYD2	I1	O1	0.795
Lignin	Lignin	HYD2	I1	O1	1.000
Heat	Electricity	TBG	I1	O1	0.750
Natural Gas	Heat	CB	I1	O1	13.880
Lignin	Lignin	AHP	I1	O1	0.784
Glucan	Glucan	AHP	I1	O2	0.950
Xylan	Xylan	AHP	I1	O2	0.548
Glucan	DGlucan	AHP	I1	O2	0.050
Xylan	DXylan	AHP	I1	O2	0.453
Lignin	Lignin	AHP	I1	O2	0.216

Table S2 (continued)**.** Conversion coefficient of each block, Related to **Figure 1.**

i	*i'*	*j*	*pn*	*pn*	$\eta_{i,p,i',p'}$
Glucan	Glucose	HYD3	I1	O1	1.089
Xylan	Xylose	HYD3	I1	O1	1.057
DGlucan	Glucose	HYD3	I1	O1	1.111
DXylan	Xylose	HYD3	I1	O1	1.136
Lignin	Lignin	HYD3	I1	O1	1.000
Glucan	Glucan	HYD3	I1	O1	0.010
Xylan	Xylan	HYD3	I1	O1	0.050
Lignin	Lignin	EA	I1	O1	0.440
Glucan	Glucan	EA	I1	O2	0.960
Xylan	Xylan	EA	I1	O2	0.960
Glucan	DGlucan	EA	I1	O2	0.040
Xylan	DXylan	EA	I1	O2	0.040
Lignin	Lignin	EA	I1	O2	0.560
Glucan	Glucose	HYD4	I1	O1	1.044
Xylan	Xylose	HYD4	I1	O1	0.966
DGlucan	Glucose	HYD4	I1	O1	1.111
DXylan	Xylose	HYD4	I1	O1	1.136
Lignin	Lignin	HYD4	I1	O1	1.000
Glucan	Glucan	HYD4	I1	O1	0.060
Xylan	Xylan	HYD4	I1	O1	0.150
Lignin	Lignin	GVL	I1	O1	0.830
Glucan	Glucan	GVL	I1	O1	0.120
Xylan	Xylan	GVL	I1	O1	0.170
Glucan	Glucose	GVL	I1	O2	0.800
Xylan	Xylose	GVL	I1	O2	0.750
Glucose	Glucose	COFER2	I1	O1	0.130
Xylose	Xylose	COFER2	I1	O1	0.130
Glucose	Ethanol	COFER2	I1	O1	0.485
Xylose	Ethanol	COFER2	I1	O1	0.485
Glucose	Glucose	SEP2	I1	O2	1.000
Xylose	Xylose	SEP2	I1	O2	1.000
Ethanol	Ethanol	SEP2	I1	O1	0.990

Table S3. Unit heat and electricity requirement, and unit production cost of different blocks, Related to **Figure 1.**

Block	Heat $\mu_{i=\text{heat},j}$ (kWh kg^{-1})	Electricity $\mu_{i=\text{electricity},j}$ (kWh kg^{-1})	Production Cost θ_j ($ kg^{-1} or *$ kWh^{-1})	Reference
DA	0.737	0.086	0.050	Humbird et al., 2011
AFEX	0.664	0.090	0.030	Kazi et al., 2010
HYD1	0.008	0.080	0.044	Humbird et al., 2011
HYD2	0.020	0.120	0.044	Kazi et al., 2010
SSCF	0.008	0.142	0.028	Aden et al., 2002
COFER1	-	0.045	0.060	Humbird et al., 2011
SEP1	1.050	0.054	0.025	Humbird et al., 2011
WWT	0.004	1.830	0.400	Humbird et al., 2011
LV	2.700	0.050	0.162	Ng et al., 2019
CB	-	0.058	0.060	Humbird et al., 2011
TBG	-	-	0.008*	Humbird et al., 2011
EA	2.447	0.138	0.040	Da Costa Sousa et al., 2016
AHP	0.250	0.040	0.219	Bhalla et al., 2018
HYD3	0.008	0.091	0.046	Bhalla et al., 2018
HYD4	0.008	0.091	0.046	Bhalla et al., 2018
SEP2	0.500	0.030	0.020	Won et al., 2017
COFER2	0.555	0.030	0.045	Won et al., 2017
GVL	1.000	0.080	0.051	Won et al., 2017
SV	5.000	0.060	0.600	Ng et al., 2019

Transparent Methods

Optimization-based Process Synthesis

Optimization-based synthesis involves three major steps: (1) constructing a superstructure with possible process alternatives, (2) formulating an optimization model representing mass and energy balances of the underlying systems, and (3) solving the resulting model to determine the optimal configuration and processing conditions (Wu et al., 2016). Consider a generic superstructure (**see Figure S1**) consisting of four major elements:

(1) Block: has one or more operations/technologies (e.g., fermentation, hydrolysis, separation, etc).

(2) Port: corresponds to stream inlet/outlet point of each block. An inlet port merges substreams from different outlet ports into a parent stream for entering a block, while an outlet port splits the parent stream leaving a block into substreams that flow to different inlet ports (Wu et al., 2016). In particular, a block can have multiple outlet port, but only one inlet port.

(3) Stream: connects an outlet and inlet port.

(4) Component: consists of all chemical components to be included in the studied process. The component flow is carried by each stream.

In this work, each block has a set of technical (conversion coefficient), economic (unit conversion cost), and energy (heat and electricity requirement) parameters, which are obtained from the literature or using simple process models (see the details in the next section "Parameter Determination"). Note that the unit conversion cost has capital, fixed and variable operating cost components. Lower and upper capacity bounds are also defined. For sources and sinks, we obtain the components' unit prices, as well as their minimum and maximum supplies or demands.

Parameter Determination

We first assume the market price of feedstocks, resources, products, and by-products can be found from literature (Bhalla et al., 2018; da Costa Sousa et al., 2016; Humbird et al., 2011; Kazi et al., 2010; Ng et al., 2019; US Environmental Protection Agency, 2018; Won et al., 2017) (**Table S1**). All costs are indexed to 2017 US dollars and calculated based on a dry mass basis.

Next, we calculate conversion coefficients based on the components exist in the inlet and outlet flows of the block (**Table S2**). Note that auxiliary inputs (e.g., water, catalyst, enzymes, etc.) do not appear as components in the superstructure, thus they are not included in the calculation of conversion coefficients (see (Kim et al., 2013) for more details). The unit energy consumption of each block (**Table S2**) is calculated based on the total annual energy divided by the annual consumption rate (exclude auxiliary inputs) of the block. The boiler efficiency is assumed as 80%.

We also calculate the unit production cost (**Table S3**), which has capital, fixed and variable operating cost components. The capital cost includes the costs of equipment and other miscellaneous costs, e.g., piping and instrumentation, etc. (Humbird et al., 2011). The annualized capital cost is then calculated from the capital multiplied by the capital recovery factor based on 10% of interest rates and 25 years

of plant's lifetime. The fixed operating cost includes labor charges, maintenance, etc., while the variable operating cost covers material purchase, waste handling, etc. Auxiliary inputs (e.g., water, catalyst, enzymes, etc.) are included in the calculation of operating costs. The unit production cost is calculated based on the summation of annual operating costs and annualized capital cost, divided by the annual consumption rate of the block (see (Kim et al., 2013) for more details).

Problem Statement

We consider a problem with given biomass feedstock (e.g., corn stover, switch grass or pinewood), intermediates (glucose, xylose, and lignin), products (e.g., ethanol, bioproducts, and electricity), as well as external resources (e.g., natural gas and electricity) which are available to purchase if needed. The unit prices of biomass feedstock, products, by-products, and external resources are known. A set of blocks (pretreatment, hydrolysis, fermentation, separation, heat and power generation, etc.) are defined to convert biomass feedstock into ethanol, by-products, and energy. Each block has known energy requirement, conversion efficient, and unit conversion cost. In addition, the lower and upper bounds for (1) capacity of the block, (2) biomass feedstock availability and external resource supplies, and (3) product and by-product demands are also predetermined. We aim to identify the least cost strategy to produce one kg of ethanol. The optimization model has decision variables, such as the material and energy flow of each block, the feedstock and external resources purchase, and the by-product sales.

Biorefinery Superstructure

Figure 1 shows the superstructure for the conversion of corn stover to ethanol (Ng et al., 2019). The corn stover feedstock, consisting of glucan, xylan, and lignin, can be sent to five candidate pretreatment blocks (e.g., dilute acid-based (DA), ammonia fiber expansion-based (AFEX), copper-catalyzed alkaline hydrogen peroxide-based (AHP) (Bhalla et al., 2018), extractive ammonia-based (EA), and γ-valerolactone-based (GVL)). The effluent of the pretreatment block is fed to corresponding hydrolysis and fermentation blocks (e.g., simultaneous saccharification and co-fermentation (SSCF), co-fermentation (COFER1)), to produce sugars (e.g., glucose and xylose) from glucan and xylan. The produced sugars are converted to ethanol. Ethanol is then recovered from water, stillage (glucose and xylose), and solid residues in the separation block (SEP1).

Stillage can be utilized either in the valorization block (SV) to produce and recover value-added bioproducts or in the wastewater treatment block (WWT) to produce biogas. Similarly, solid residues (mainly lignin) can be valorized (LV) to produce value-added bioproducts and/or combusted with biogas from SV in the combustor and boiler (CB) to generate heat. Excessive heat is used to generate electricity in the turbogenerator (TBG). External resources (e.g., natural gas, electricity, etc.) can be purchased if the generated heat and power are not sufficient (i.e., the biorefinery is "energy-deficient".) to satisfy the energy requirement in the biorefinery. Note that both SV and LV blocks have considered the units required for the separation and recovery of high purity bioproducts.

The GVL block includes both conversion and separation; and has two outlet streams: sugars and solid residues. The former is sent to co-fermentation (COFER2) and the subsequent separation (SEP2) directly, while the latter is sent for lignin valorization (LV) and/or heat generation (CB).

All parameter data are provided in the Supplementary Material. All costs are indexed to 2017 US dollars and calculated based on a dry mass basis. The objective function is to minimize the total cost to produce 1 kg of ethanol, which includes the feedstock and additional resource purchases, and the production costs, minus the sales of by-products. Thus, the minimum ethanol cost is equivalent to the minimum ethanol selling price (MESP, the breakeven selling price that leads to zero net present value). The mixed-integer linear programming (MINLP) model is subject to material and energy balance, and constraints that are presented in Supplemental Material. We use GAMS 25.1 with BARON as the global MINLP solver.

Mathematical Formulation

Formally, the problem is stated in terms of the following sets and subsets:

a) Components $i \in \mathbf{I}$.
   - $\mathbf{I}^{\mathrm{F}}$: biomass feedstocks; $\mathbf{I}^{\mathrm{R}}$: resources; $\mathbf{I}^{\mathrm{I}}$: intermediates; $\mathbf{I}^{\mathrm{E}}$: energy; $\mathbf{I}^{\mathrm{P}}$: products; $\mathbf{I}^{\mathrm{B}}$: by-products.

b) Blocks $j \in \mathbf{J}$.
   - $\mathbf{J}^{\mathrm{PRE}}$: pretreatment; $\mathbf{J}^{\mathrm{HYD}}$ = hydrolysis; $\mathbf{J}^{\mathrm{FER}}$ = fermentation; $\mathbf{J}^{\mathrm{SEP}}$ = separation; $\mathbf{J}^{\mathrm{SV}}$ = stillage valorization; $\mathbf{J}^{\mathrm{LV}}$ = lignin valorization; $\mathbf{J}^{\mathrm{WWT}}$ = wastewater treatment; $\mathbf{J}^{\mathrm{CB}}$ = combustor and boiler; $\mathbf{J}^{\mathrm{TBG}}$ = turbogenerator.

c) Port numbers $pn \in \mathbf{PN}$.
   - $\mathbf{PN}^{\mathrm{IN}}$: inlet port number; $\mathbf{PN}^{\mathrm{OUT}}$ = outlet port number.

d) Ports $p \in \mathbf{P} \subset \mathbf{J} \times \mathbf{PN}$, which is indexed by block and port number.
   - $\mathbf{P}^{\mathrm{IN}}$: inlet ports; $\mathbf{P}^{\mathrm{OUT}}$: outlet ports; $\mathbf{P}_j^{\mathrm{IN}}$: inlet ports of block j; $\mathbf{P}_j^{\mathrm{OUT}}$: outlet ports of block j.

e) Streams $s \in \mathbf{S} \subset \mathbf{P} \times \mathbf{P}$, which is indexed by two ports.
   - $\mathbf{S}_{p'}$: streams originating from outlet port p'; $\mathbf{S}_j$: streams that are connected to block j.

The binary parameters $\chi_{i,p',p}$ can be predefined for the component i present in the stream from outlet port p' and inlet port p after the superstructure is generated. The examples of sets, subsets and binary parameters are shown in **Figure S2A**. For example, the stream between outlet port P3 and inlet port P5 does not contain component Cc, therefore $\chi_{\mathrm{Cc,P3,P5}} = 0$.

The parameters are given as follows:

- λ_i: unit price of components $i \in \mathbf{I}^{\mathrm{F}} \cup \mathbf{I}^{\mathrm{R}} \cup \mathbf{I}^{\mathrm{P}} \cup \mathbf{I}^{\mathrm{B}}$ (\$ kg^{-1} or \$ kWh^{-1}).
- $\underline{\varrho}_i / \overline{\varrho}_i$: minimum/maximum supply of components $i \in \mathbf{I}^{\mathrm{F}} \cup \mathbf{I}^{\mathrm{R}}$ (kg or kWh).
- $\underline{\rho}_i / \overline{\rho}_i$: minimum/maximum demand of components $i \in \mathbf{I}^{\mathrm{P}} \cup \mathbf{I}^{\mathrm{B}}$ (kg or kWh).
- $\underline{\zeta}_j / \overline{\zeta}_j$: lower/upper capacity bounds of block j (kg or kWh).

- $\mu_{i,j}$: unit energy $i \in \mathbf{I}^{\mathrm{E}}$ (heat and electricity) requirement of block j (kWh kg^{-1}).
- $\eta_{i,p,i',p'}$: conversion coefficient (kg kg^{-1} or kWh kg^{-1} or kWh kWh^{-1}).
- θ_j: unit production cost of block j (\$ kg^{-1} or \$ kWh^{-1}).
- κ: boiler efficiency.

Variable $Y_j \in \{0,1\}$, which is equal to 1 if block j is selected, and the following nonnegative continuous variables are introduced:

- $E^{\mathrm{C}}_{i\,p',p}$: energy flow between outlet port p' and inlet port p (kWh).
- $E^{\mathrm{IN}}_{i,p}/E^{\mathrm{OUT}}_{i,p'}$: inlet/outlet energy flow (kWh).
- $E^{\mathrm{SR}}_{i}/E^{\mathrm{SK}}_{i}$: energy flow from/towards source/sink (kWh).
- $E^{\mathrm{UT}}_{i}/E^{\mathrm{W}}$: total energy requirement of biorefinery/waste heat (kWh).
- $F^{\mathrm{C}}_{i,\,p',p}$: mass flow between outlet port p' and inlet port p (kg).
- $F^{\mathrm{IN}}_{i,p}/F^{\mathrm{OUT}}_{i,p'}$: inlet/outlet mass flow (kg).
- $F^{\mathrm{SR}}_{i}/F^{\mathrm{SK}}_{i}$: mass flow from/towards source/sink (kg).
- $R_{p',p}$: split fraction of stream between outlet port p' and inlet port p.
- X_j: total consumption level of block j (kg).
- Z: total cost (\$).

Material Balance

The feedstock flow is converted into flows of the major constituent of biomass (e.g., glucan, xylan, and lignin) through a dummy conversion block (**Figure S2B**) modeled as follows:

$$\sum_{i\in\mathbf{I}^{\mathrm{F}}} \eta_{i,p''=\mathrm{DFI},i',p'=\mathrm{DFO}} F^{\mathrm{SR}}_{i} = \sum_{j\in\mathbf{J}^{\mathrm{PRE}},p\in\mathbf{P}^{\mathrm{IN}}_{j}} F^{\mathrm{C}}_{i',p'=\mathrm{DFO},p} \qquad \forall i' \in \mathbf{I}^{\mathrm{I}} \tag{1}$$

where $\eta_{i,p'',i',p'}$ in this equation corresponds to the composition of biomass feedstock. DFI and DFO are dummy inlet port and outlet port, respectively (see **Figure S2B**).

The inlet mass flow $F^{\mathrm{IN}}_{i,p}$ (**Figure S2C**) is given as:

$$F^{\mathrm{IN}}_{i,p} = \sum_{p'\in\mathbf{P}^{\mathrm{OUT}}|\chi_{i,p',p}=1} F^{\mathrm{C}}_{i,\,p',p} \qquad \forall i \in \mathbf{I}^{\mathrm{I}}, j \in \mathbf{J}\setminus\mathbf{J}^{\mathrm{TBG}}, p \in \mathbf{P}^{\mathrm{IN}}_{j} \tag{2}$$

where $F^{\mathrm{C}}_{i,\,p',p}$ is the connecting flow between outlet and inlet ports.

The outlet mass flow $F^{\mathrm{OUT}}_{i',p'}$ is given as:

$$F^{\mathrm{OUT}}_{i',p'} = \sum_{i\in\mathbf{I}^{\mathrm{I}},p\in\mathbf{P}^{\mathrm{IN}}_{j}} \eta_{i,p,i',p'} F^{\mathrm{IN}}_{i,p} \qquad \forall i' \in \mathbf{I}^{\mathrm{I}}, j \in \mathbf{J}\setminus\left(\mathbf{J}^{\mathrm{CB}}\cup\mathbf{J}^{\mathrm{TBG}}\right), p' \in \mathbf{P}^{\mathrm{OUT}}_{j} \tag{3}$$

where $\eta_{i,p,i',p'}$ is a conversion coefficient.

The outlet mass flow is split at the outlet port:

$$F^{\mathrm{OUT}}_{i,p'} = \sum_{p\in\mathbf{P}^{\mathrm{IN}}|\chi_{i,p',p}=1} F^{\mathrm{C}}_{i,\,p',p} \qquad \forall i \in \mathbf{I}^{\mathrm{I}}, j \in \mathbf{J}\setminus\left(\mathbf{J}^{\mathrm{CB}}\cup\mathbf{J}^{\mathrm{TBG}}\right), p' \in \mathbf{P}^{\mathrm{OUT}}_{j} \tag{4}$$

The split fraction $R_{p',p}$ is introduced to denote the fraction of stream leaving outlet port p' and entering inlet port p to ensure that the component concentrations in all outgoing streams are the same:

$$F_{i,p'}^{\mathrm{OUT}} R_{p',p} = F_{i,p',p}^{\mathrm{C}} \qquad \forall i \in \mathbf{I}^{\mathrm{I}}, p', p | \chi_{i,p',p} = 1 \tag{5}$$

$R_{p,p'}$ is constrained by the following equations:

$$0 \le R_{p',p} \le Y_j \qquad \forall j, (p', p) \in \mathbf{S}_j \tag{6}$$

$$\sum_{p \in \mathbf{S}_{p'}} R_{p',p} = Y_j \qquad \forall j, p' \in \mathbf{P}_j^{\mathrm{OUT}} \tag{7}$$

where Y_j is the binary variable for the selection of block j.

The mass inflow towards sink (e.g., product and by-product) F_i^{SK} is given as:

$$F_i^{\mathrm{SK}} = \sum_{p' \in \mathbf{P}^{\mathrm{OUT}} | \chi_{i,p',p=\mathrm{DPBI}}=1} F_{i,p',p=\mathrm{DPBI}}^{\mathrm{C}} \qquad \forall i \in \mathbf{I}^{\mathrm{P}} \cup \mathbf{I}^{\mathrm{B}} \tag{8}$$

where DPBI is the dummy inlet port of a dummy conversion block (see **Figure S2D**).

Additional resources (e.g., natural gas) can also be fed to the CB blocks (see **Figure S2E**):

$$F_i^{\mathrm{SR}} = \sum_{j \in \mathbf{J}^{\mathrm{CB}}, p \in \mathbf{P}_j^{\mathrm{IN}}} F_{i,p}^{\mathrm{IN}} \qquad \forall i \in \mathbf{I}^{\mathrm{R}} \tag{9}$$

Energy Balance

The heat generated from the CB blocks $E_{i'=\mathrm{heat},p'}^{\mathrm{OUT}}$ is given as:

$$E_{i'=\mathrm{heat},p'}^{\mathrm{OUT}} = \sum_{i \in \mathbf{I}^{\mathrm{I}} \cup \mathbf{I}^{\mathrm{R}}, p \in \mathbf{P}_j^{\mathrm{IN}}} \eta_{i,p,i'=\mathrm{heat},p'} F_{i,p}^{\mathrm{IN}} \qquad \forall j \in \mathbf{J}^{\mathrm{CB}}, p' \in \mathbf{P}_j^{\mathrm{OUT}} \tag{10}$$

After considering boiler efficiency κ, the heat balance is:

$$\kappa E_{i=\mathrm{heat},p'}^{\mathrm{OUT}} = E_{i=\mathrm{heat}}^{\mathrm{UT}} + E^{\mathrm{W}} + \sum_{p \in \mathbf{P}^{\mathrm{IN}} | \chi_{i=\mathrm{heat},p',p}=1} E_{i=\mathrm{heat},p',p}^{\mathrm{C}} \quad \forall j \in \mathbf{J}^{\mathrm{CB}}, p' \in \mathbf{P}_j^{\mathrm{OUT}} \tag{11}$$

where E_i^{UT} is the total energy (heat/electricity) requirement at the biorefinery; E^{W} is waste heat if no turbogenerator is selected; $E_{i,p',p}^{\mathrm{C}}$ is the connecting energy flow between two ports. E_i^{UT} is determined in the following equation:

$$E_i^{\mathrm{UT}} = \sum_j \mu_{i,j} X_j \qquad \forall i \in \mathbf{I}^{\mathrm{E}} \tag{12}$$

where $\mu_{i,j}$ is the unit energy requirement of each block j and X_j is the total consumption level of block j, which is given as:

$$X_j = \sum_{i \in \mathbf{I}^{\mathrm{I}} \cup \mathbf{I}^{\mathrm{R}} \setminus \mathbf{I}^{\mathrm{E}}, p \in \mathbf{P}_j^{\mathrm{IN}}} F_{i,p}^{\mathrm{IN}} \qquad \forall j \in \mathbf{J} \setminus \mathbf{J}^{\mathrm{TBG}} \tag{13}$$

$$X_j = \sum_{i \in \mathbf{I}^{\mathrm{E}}, p \in \mathbf{P}_j^{\mathrm{IN}}} E_{i,p}^{\mathrm{IN}} \qquad \forall j \in \mathbf{J}^{\mathrm{TBG}} \tag{14}$$

The heat inlet flow at the TBG blocks $E_{i,p}^{\mathrm{IN}}$ (**Figure S2E**) is given as:

$$E_{i=\mathrm{heat},p}^{\mathrm{IN}} = \sum_{p' \in \mathbf{P}^{\mathrm{OUT}} | \chi_{i=\mathrm{heat},p',p}=1} E_{i=\mathrm{heat},p',p}^{\mathrm{C}} \qquad \forall j \in \mathbf{J}^{\mathrm{TBG}}, p \in \mathbf{P}_j^{\mathrm{IN}} \tag{15}$$

The electricity generated by the TBG block $E_{i=\mathrm{electricity},p'}^{\mathrm{OUT}}$ is given as:

$$E^{\mathrm{OUT}}_{i'=\mathrm{electricity},p'} = \sum_{p\in\mathbf{P}^{\mathrm{IN}}_j} \eta_{i=\mathrm{heat},p,i'=\mathrm{electricity},p'} E^{\mathrm{IN}}_{i=\mathrm{heat},p} \qquad \forall j \in \mathbf{J}^{\mathrm{TBG}}, p' \in \mathbf{P}^{\mathrm{OUT}}_j \tag{16}$$

The electricity balance is given as:

$$\sum_{j\in\mathbf{J}^{\mathrm{TBG}},p'\in\mathbf{P}^{\mathrm{OUT}}_j} E^{\mathrm{OUT}}_{i=\mathrm{electricity},p'} + E^{\mathrm{SR}}_{i=\mathrm{electricity}} = E^{\mathrm{UT}}_{i=\mathrm{electricity}} + E^{\mathrm{SK}}_{i=\mathrm{electricity}} \tag{17}$$

where electricity E^{SR}_i and E^{SK}_i can be purchased and sold from and to the market, respectively.

Bounds

The product and by-product are bounded as follows:

$$\underline{\rho}_i \le F^{\mathrm{SK}}_i \le \overline{\rho}_i \qquad \forall i \in \mathbf{I}^{\mathrm{P}} \cup \mathbf{I}^{\mathrm{B}} \setminus \mathbf{I}^{\mathrm{E}} \tag{18}$$

$$\underline{\rho}_i \le E^{\mathrm{SK}}_i \le \overline{\rho}_i \qquad \forall i \in \mathbf{I}^{\mathrm{B}} \cap \mathbf{I}^{\mathrm{E}} \tag{19}$$

Similarly, the feedstock and resource flows are bounded as follows:

$$\underline{\varrho}_i \le F^{\mathrm{SR}}_i \le \overline{\varrho}_i \qquad \forall i \in \mathbf{I}^{\mathrm{F}} \cup \mathbf{I}^{\mathrm{R}} \setminus \mathbf{I}^{\mathrm{E}} \tag{20}$$

$$\underline{\varrho}_i \le E^{\mathrm{SR}}_i \le \overline{\varrho}_i \qquad \forall i \in \mathbf{I}^{\mathrm{R}} \cap \mathbf{I}^{\mathrm{E}} \tag{21}$$

The consumption level is bounded by:

$$\underline{\zeta}_j Y_j \le X_j \le \overline{\zeta}_j Y_j \qquad \forall j \tag{22}$$

The following constraints enforce the number of blocks to be selected:

$$\sum_{j\in\boldsymbol{J}^{\mathrm{PRE}}} Y_j = 1, \sum_{j\in\boldsymbol{J}^{\mathrm{HYD}}} Y_j \le 1, \sum_{j\in\boldsymbol{J}^{\mathrm{FER}}} Y_j = 1, \sum_{j\in\boldsymbol{J}^{\mathrm{SEP}}} Y_j = 1, \sum_{j\in\boldsymbol{J}^{\mathrm{WWT}}} Y_j = 1, \sum_{j\in\boldsymbol{J}^{\mathrm{CB}}} Y_j = 1 \tag{23}$$

Objective Function

The objective is to minimize the total cost, which includes the feedstock and additional resource purchases, and the total production cost of the biorefinery, minus the sales of by-products.

$$\mathrm{Min}\ Z = \left(\sum_{i\in\mathbf{I}^{\mathrm{F}}\cup\mathbf{I}^{\mathrm{R}}\setminus\mathbf{I}^{\mathrm{E}}} \lambda_i F^{\mathrm{SR}}_i + \sum_{i\in\mathbf{I}^{\mathrm{R}}\cap\mathbf{I}^{\mathrm{E}}} \lambda_i E^{\mathrm{SR}}_i\right) + \sum_j \theta_j X_j - \left(\sum_{i\in\mathbf{I}^{\mathrm{B}}\setminus\mathbf{I}^{\mathrm{E}}} \lambda_i F^{\mathrm{SK}}_i + \sum_{i\in\mathbf{I}^{\mathrm{B}}\cap\mathbf{I}^{\mathrm{E}}} \lambda_i E^{\mathrm{SK}}_i\right) \tag{24}$$

where λ_i is the unit price of components i and θ_j is the unit production cost of blocks j.

Note that the formulations are linear, except the bilinearities in Equation 5. The MINLP model is implemented in GAMS and solved using BARON.

Impact of Uncertainty: Major Parameters Not Describing Lignin Valorization

We study the impact of uncertainty in four parameters (feedstock price, electricity price, production cost, and lignin conversion coefficient in pretreatment) on the ethanol production cost in the base case design (S^{BC}). Specifically, we calculate the cost for 5,000 randomly generated scenarios, where, in each scenario, a value for each one of these four parameters is sampled from the corresponding (triangular) distribution. The assumptions for these distributions are taken from: (A) Feedstock price (Huang et al., 2018), (B) electricity export price (2002-2018 United States industrial average retail price of electricity from U.S. Energy Information Administration), (C) Production cost variation (Merrow et al., 1981), and (D) Lignin conversion coefficient in GVL block (Won et al., 2017). The

parameters of the distributions as well as the histograms of the values used in our evaluation are shown in **Figure S3**. The optimization model is run for each one of the scenarios, and the distribution of the resulting minimum ethanol cost is shown in **Figure S4**.

The distribution in **Figure S4** suggests that the impact of uncertainty in these parameters on the minimum ethanol cost is substantial. However, this does not mean that the insights, based on the strategy transitions shown in the heat maps in the paper, will change. This is because, as explained in the main text, changes in the four parameters studied here impact both the lignin-to-heat/power and lignin-to-bioproducts strategies.

To illustrate, consider uncertainty in pretreatment (which is one of the most challenging and expensive processing steps for lignocellulosic biomass). An increase in the pretreatment cost will not necessarily change the transition of configurations shown in our figures because more expensive pretreatment means a more expensive lignin stream, regardless of where this lignin stream goes (boiler vs. valorization). It will change the minimum cost of ethanol, that is, the scale of the shown heat maps, but it will not significantly change the actual selection of the lignin valorization block, which is what we aim to study primarily. More generally, uncertainty in the processing parameters (cost, conversion, energy requirement) of almost all blocks, other than lignin valorization, is expected to have, similarly, low impact. There are two exceptions: parameters describing the conversion of lignin to (1) heat and power, and (2) valuable chemicals.

The presented analysis can be viewed as a study of a basic trade-off: benefit from using lignin to produce heat and power (current configuration) *versus* benefit from valorizing lignin. Thus, it is the uncertainty in blocks CB, TBG, LV (see **Figure 1**) that will indeed change the results. However, combustion and electricity generation from steam are well known processes and the parameters we use have little uncertainty. Thus, it the uncertainty in lignin valorization, which is at early stages of development and hence subject to significant uncertainty, that is likely to change the selection of the optimal biorefinery strategy and economics. The analysis of the paper can be viewed, precisely, as a study of the impact of uncertainty in some key LV parameters. The heat maps show how the cost and biorefinery configurations change as the values of these uncertain parameters change.

Supplemental References

Aden, A., Ruth, M., Ibsen, K., Jechura, J., Neeves, K., Sheehan, J., Wallace, B., Montague, L., Slayton, A., Lukas, J., 2002. Lignocellulosic Biomass to Ethanol Process Design and Economics Utilizing Co-Current Dilute Acid Prehydrolysis and Enzymatic Hydrolysis for Corn Stover. Golden, CO (United States).

Bhalla, A., Fasahati, P., Particka, C.A., Assad, A.E., Stoklosa, R.J., Bansal, N., Semaan, R., Saffron, C.M., Hodge, D.B., Hegg, E.L., 2018. Integrated experimental and technoeconomic evaluation of two-stage Cu-catalyzed alkaline-oxidative pretreatment of hybrid poplar. Biotechnol. Biofuels 11, 143. https://doi.org/10.1186/s13068-018-1124-x

Da Costa Sousa, L., Jin, M., Chundawat, S.P.S., Bokade, V., Tang, X., Azarpira, A., Lu, F., Avci, U., Humpula, J., Uppugundla, N., Gunawan, C., Pattathil, S., Cheh, A.M., Kothari, N., Kumar, R., Ralph, J., Hahn, M.G., Wyman, C.E., Singh, S., Simmons, B.A., Dale, B.E., Balan, V., 2016. Next-generation ammonia pretreatment enhances cellulosic biofuel production. Energy Environ. Sci. 9, 1215–1223. https://doi.org/10.1039/c5ee03051j

Huang, K., Won, W., Barnett, K.J., Brentzel, Z.J., Alonso, D.M., Huber, G.W., Dumesic, J.A., Maravelias, C.T., 2018. Improving economics of lignocellulosic biofuels: An integrated strategy for coproducing 1,5-pentanediol and ethanol. Appl. Energy 213, 585–594. https://doi.org/10.1016/j.apenergy.2017.11.002

Humbird, D., Davis, R., Tao, L., Kinchin, C., Hsu, D., Aden, A., Schoen, P., Lukas, J., Olthof, B., Worley, M., Sexton, D., Dudgeon, D., 2011. Process Design and Economics for Biochemical Conversion of Lignocellulosic Biomass to Ethanol: Dilute-Acid Pretreatment and Enzymatic Hydrolysis of Corn Stover, National Renewable Energy Laboratory (NREL). Golden, CO (United States). https://doi.org/10.2172/1013269

Kazi, F.K., Fortman, J.A., Anex, R.P., Hsu, D.D., Aden, A., Dutta, A., Kothandaraman, G., 2010. Techno-economic comparison of process technologies for biochemical ethanol production from corn stover. Fuel 89, S20–S28. https://doi.org/10.1016/j.fuel.2010.01.001

Merrow, E.W., Phillips, K., Myers, C.W., 1981. Understanding Cost Growth and Performance Shortfalls in Pioneer Process Plants. RAND Corporation, Santa Monica, CA.

Ng, R.T.L., Fasahati, P., Huang, K., Maravelias, C.T., 2019. Utilizing stillage in the biorefinery: Economic, technological and energetic analysis. Appl. Energy 241, 491–503. https://doi.org/10.1016/j.apenergy.2019.03.020

Won, W., Motagamwala, A.H., Dumesic, J.A., Maravelias, C.T., 2017. A co-solvent hydrolysis strategy for the production of biofuels: Process synthesis and technoeconomic analysis. React. Chem. Eng. 2, 397–405. https://doi.org/10.1039/c6re00227g

Wu, W.Z., Henao, C.A., Maravelias, C.T., 2016. A superstructure representation, generation, and modeling framework for chemical process synthesis. AIChE J. 62, 3199–3214. https://doi.org/10.1002/aic.15300